

Characterizing Multi-Carrier Devices with Quantitative Mobility Spectrum Analysis and Variable Field Hall Measurements

Gang Du¹, J. R. Lindemuth¹, B. C. Dodrill¹, R. Sandhu², M. Wojtowicz², Mark S. Goosky³, I. Vurgaftman⁴, J. R. Meyer⁴

¹ Lake Shore Cryotronics, Inc., 575 McCorkle Boulevard, Westerville, OH 43082, USA

² TRW, One Space Park, Redondo Beach, CA 90278, USA

³ Dept. of Material Science and Engineering, UCLA, Los Angeles, CA 90095, USA

⁴ Code 5613, Naval Research Lab, Washington, DC 20375, USA

Single magnetic field Hall measurements are inadequate for characterizing multi-carrier mixed conduction in heterostructure devices, since the resultant mobility and density parameters are averaged over all carriers. We demonstrate an optimized quantitative mobility spectrum analysis (QMSA) technique for resolving individual carrier mobilities and densities in multi-carrier devices such as *p*HEMTs from field dependent Hall measurement data. The reliability and sensitivity of this technique suggests that it is a suitable standard tool for routine characterization of multi-carrier semiconductor devices.

Introduction

Advances in compound semiconductors have resulted in novel heterostructure devices with superior performance. These devices are widely used in RF, microwave, and optical applications today. The rapid pace with which these device technologies have advanced have, in turn, necessitated the development of new measurement and data analysis techniques. For example, conventional single magnetic field Hall characterization is incapable of providing a precise determination of the electronic transport properties of a multi-layered device such as a *p*HEMT. The key parameters of a *p*HEMT are mobility and density of the 2DEG carrier (or carriers) in the quantum well channel layer. In order to characterize the 2DEG carrier in a *p*HEMT device with single field Hall measurement technique, one has to either repeat the steps of etching and characterizing until the doped cap layer is removed, or terminate the epi growth process before the cap layer is formed. Even if these steps are taken, the accuracy of the characterization cannot be guaranteed if additional carrier(s) such as surface and interface charges exist in the measured sample.

In this paper, we demonstrate a novel multi-carrier characterization technique, the quantitative mobility spectrum analysis (QMSA),¹⁻⁶ which is an improvement over previous spectrum data analysis approaches.^{7,8} Similar to two other mixed conduction analysis techniques, finite number carrier least-square fit⁹ and Shubnikov-de Haas (SdH) effect,¹⁰ this technique analyzes variable magnetic field Hall data. QMSA complements these two methods, but also provides significant advantages. For example, the finite number carrier fit method requires knowledge of the number of carriers in advance, whereas fully automated QMSA requires no advance sample information and is capable of providing mobilities and densities with accuracy comparable to the finite number fit technique. Although the SdH technique can in some cases extract individual carrier densities in a multi-carrier sample that displays multiple oscillation periods, unlike QMSA it cannot provide mobility values.

In this work, we apply QMSA to synthetic multi-carrier Hall data, and also to variable field Hall measurement data for an InP *p*HEMT device from TRW. The results show that this technique extracts individual carrier mobilities and densities for multi-carrier materials, and is especially reliable and sensitive for high mobility heterostructure devices such as *p*HEMTs. Comparison with the results of SdH measurements will be discussed.

QMSA

1. Theoretical background

For a single carrier material, the measured Hall coefficient and resistivity are given by,¹¹

$$R_H(B) = \frac{1}{nq} \quad (1)$$

$$r(B) = \frac{1}{nq\mathbf{m}}, \quad (2)$$

and the conductivity tensor is given by,

$$\mathbf{s}_{xx} = \frac{nq\mathbf{m}}{1 + \mathbf{m}^2 B^2} \quad (3)$$

$$\mathbf{s}_{xy} = \frac{nq\mathbf{m}^2 B}{1 + \mathbf{m}^2 B^2}. \quad (4)$$

Here n is the carrier concentration, \mathbf{m} is the mobility, q is the charge of the carrier, and B is the magnetic field. It is apparent from Eqs. (1) and (2) that for single carrier materials the Hall

coefficient and resistivity are field independent. The single field Hall characterization is therefore sufficient for such materials.

However, for multi-carrier systems the mobility and density calculated from Eqs. (1) and (2) will be averaged over all carriers. For such materials, conductivities of the individual carriers are additive, and the total conductivity tensor (of a N -carrier system) is given by:²

$$\mathbf{s}_{xx} = \sum_i^N \frac{n_i q_i \mathbf{m}_i}{1 + \mathbf{m}_i^2 B^2} \quad (5)$$

$$\mathbf{s}_{xy} = \sum_i^N \frac{n_i q_i \mathbf{m}_i^2 B}{1 + \mathbf{m}_i^2 B^2} \quad (6)$$

The finite number carrier analysis performs a least-square fit of the measured data to a preset number of carriers:

$$\mathbf{c}^2 = \sum_i^M [(\mathbf{s}_{xx}^{\text{exp}}(B_i) - \sum_j^N \mathbf{s}_{xx}^j(B_i))^2 + (\mathbf{s}_{xy}^{\text{exp}}(B_i) - \sum_j^N \mathbf{s}_{xy}^j(B_i))^2], \quad (7)$$

where M is the number of data points. In this approach, the number of carriers N must be defined in advance and (\mathbf{m}_j, n_j) of each carrier are fitting parameters.

This shortcoming can be overcome by using the "mobility spectrum" concept. In this approach, discrete carriers are generalized by a conductivity density function that spreads over a continuous mobility range. The conductivity tensor is given by:¹²

$$\mathbf{s}_{xx} = \int_{-\infty}^{\infty} \frac{s^p(\mathbf{m}) + s^n(\mathbf{m})}{1 + \mathbf{m}^2 B^2} d\mathbf{m} \quad (8)$$

$$\mathbf{s}_{xy} = \int_{-\infty}^{\infty} \frac{(s^p(\mathbf{m}) - s^n(\mathbf{m})) \mathbf{m} B}{1 + \mathbf{m}^2 B^2} d\mathbf{m}, \quad (9)$$

where $s^p(\mathbf{m})$, $s^n(\mathbf{m})$ are hole and electron conductivity density functions, respectively. The QMSA analysis technique improves greatly over earlier efforts utilizing the spectrum concept.^{7,8} For detailed discussions of QMSA and its applications, please refer to References 1-6.

2. A two-carrier test of QMSA

Figure 1a shows synthetic Hall data for a two-electron-carrier case over the magnetic field range 0.005 - 5 T. The mobilities and densities of the two electron carriers are listed in Fig. 1a. A random uncertainty of 0.05% is added to the data. A single field measurement at 0.35 T

(using the data from Fig. 1a) would have yielded a mobility of $-3.98 \times 10^3 \text{ cm}^2/\text{Vs}$ and density of $-4.47 \times 10^{13} \text{ cm}^{-3}$, which clearly do not reflect either of the two carriers.

Figure 1b plots the QMSA spectrum result for this example. Two well-separated electron peaks representing the two carriers are shown in the spectrum. The mobility and density values (listed in Fig. 1b) of these two peaks extracted by QMSA match the two set carriers to within 1%.

Fig. 1b also shows a small hole peak. This is an analysis artifact due to the limited field range and measurement uncertainty. Increasing the range of magnetic fields over which measurements are conducted tends to minimize the occurrence of such artifacts. Furthermore, these artifacts are usually much smaller in magnitude than the dominant peaks and their contribution to the over all conductivity is negligible.

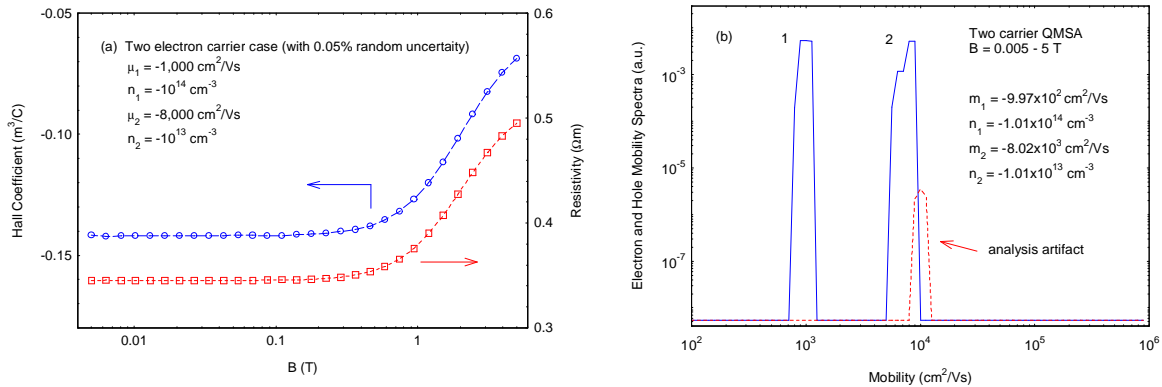


Figure 1. (a) Synthetic Hall data of the two-carrier case. (b) QMSA spectrum results of this case. Solid curve is for electrons and dashed curve is for holes (same for all the QMSA plots below).

3. A four-carrier test of QMSA

Figure 2 plots the QMSA spectrum result for a synthetic four-carrier case (three electrons and one hole with random uncertainty of 0.05%). The magnetic field range for this data set extends from 0.009 to 9 T. In addition to minimizing the artifacts discussed above, a higher field strength is needed to improve the QMSA resolution when a large number of carriers are present, particularly when their mobilities are similar in value. For this model case, all four carriers are readily extracted by QMSA. The set mobilities and densities of the four carriers and the corresponding QMSA results are listed in Table I. The accuracy of the QMSA results in this case is slightly poorer than in the two-carrier case, but is still quite reasonable.

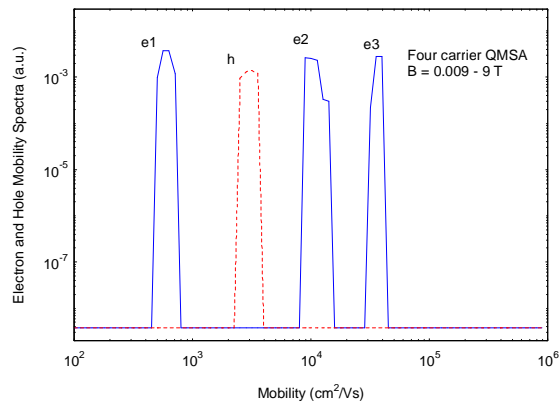


Figure 2. Four carrier case QMSA spectrum.

Table I. Four carrier case set mobilities and densities and their corresponding QMSA results.

Carrier	μ_{set} (cm ² /Vs)	μ_{QMSA} (cm ² /Vs)	n_{set} (cm ⁻³)	n_{QMSA} (cm ⁻³)
e1	-600	-601	-1e14	-1.00e14
e2	-1e4	-1.02e4	-5e12	-5.01e12
e3	-3.7e4	-3.75e4	-1e12	-9.66e11
h	3e3	3.03e3	1e13	1.00e13

Experiment

Variable field Hall and SdH measurements were conducted on an InP PHEMT device (without a cap layer) fabricated by TRW, using the Lake Shore Hall Measurement System (HMS) Model 9509. HMS 9509 is a superconducting cryogenic system with a maximum field of 9 T and temperature range of 2 - 400 K.

A Hall bar sample configuration with six contacts was used to conduct the measurements. Gold wires were heat-bonded to gold contact pads, providing ohmic contacts as assured via two-probe I-V curve measurements, which were linear.

Measurement results

1. Variable field Hall measurements and QMSA results

Variable field Hall measurements were conducted for fields from 200 G to 85 KG (0.02 to 8.5 T) and at various temperatures. Figure 3 shows the measured sheet Hall coefficient and sheet resistivity data at 100 K and 300 K. The apparent field dependence of these data

reveals the multi-carrier nature of this sample. Figure 4 shows the derived conductivity tensor and the fitted results from QMSA. The near perfect fit (solid lines) to the data is a good indication of the validity of the QMSA spectrum results presented below.

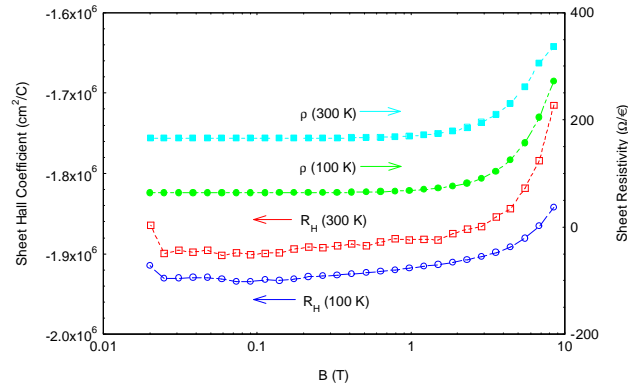


Figure 3. Variable field Hall data at 100 K and 300 K.

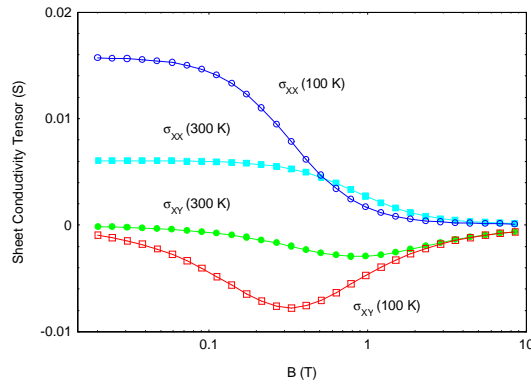


Figure 4. Derived (markers) and fitted (solid lines) conductivity tensor results at 100 K and 300 K.

Application of QMSA to the measured Hall data shown in Fig. 3 results in the multi-carrier mobility spectra plotted in Figure 5. Since this sample was grown without a doped cap layer, one might have thought that the Hall data would show only a single 2DEG carrier. However, Fig. 5 clearly shows at least two electron peaks in all plots, indicating that this sample contains at least two electron carriers. At 50 K, the high mobility electron peak is broad and has three shoulder features (indicated by the arrows in the figure). With increasing temperature, the lowest mobility feature separates from the broad peak. The two highest mobility features never separated because their mobilities are similar. These features suggest the occupation of multiple subbands in the quantum well channel layer (this assertion is substantiated by the SdH data presented below). However, at 250 K and above there is only a single combined high mobility electron peak, possibly indicating that increased electron-phonon scattering eliminates the differences in mobilities for the various subbands at higher temperatures.

The mobility of the highest mobility peak increases with decreasing temperature, indicating that electron-phonon scattering dominates the charge transport in the channel layer. Figure 6 shows the temperature dependence of the mobility for this peak.

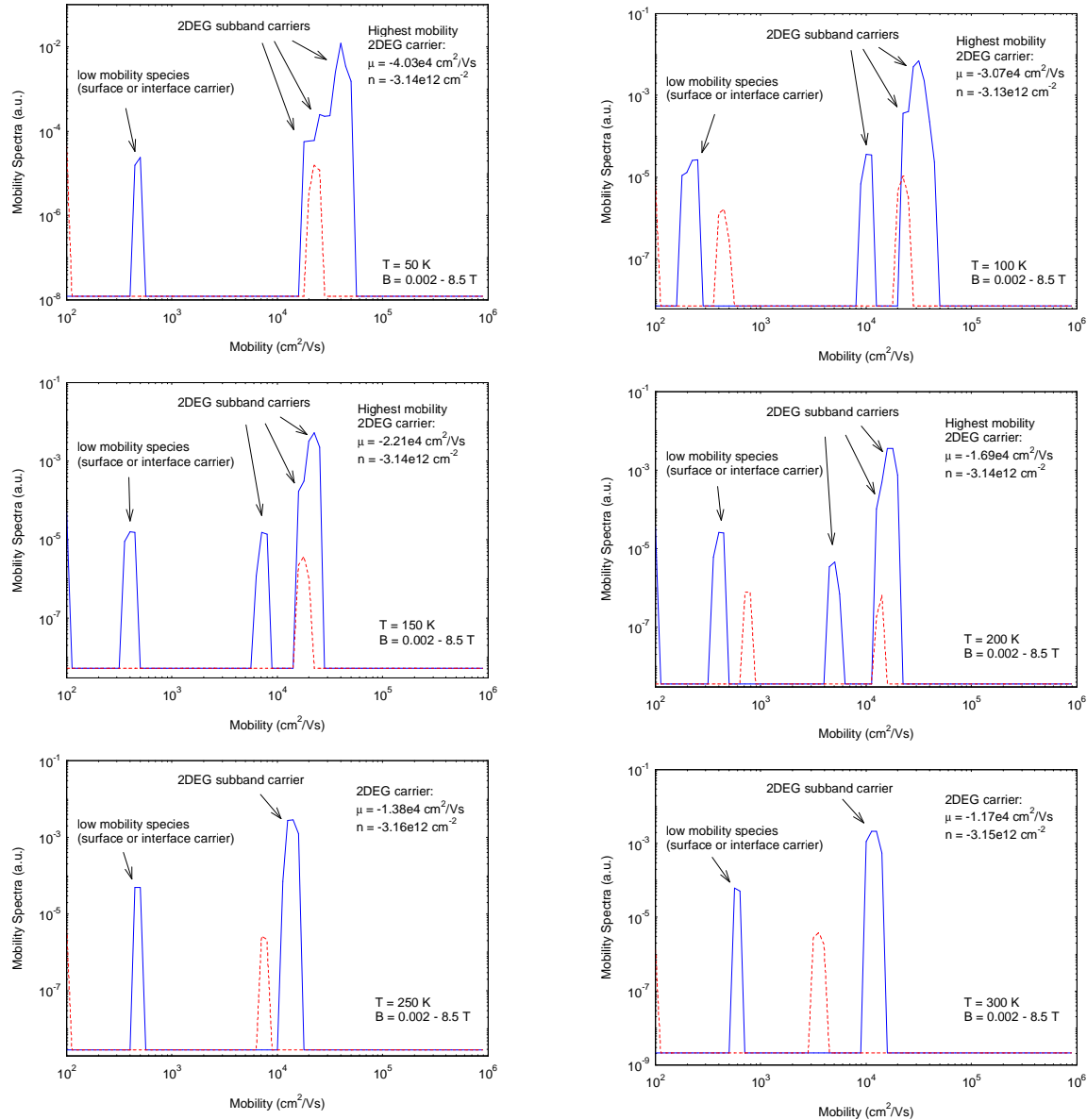


Figure 5. QMSA spectra of the InP *p*HEMT device at several temperatures. Mobility values listed are that of the highest mobility 2DEG carrier. Density values are that of the highest mobility electron peak.

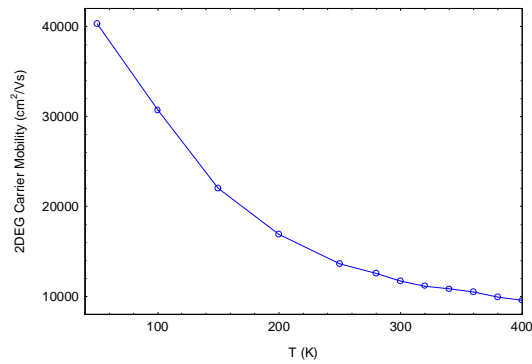


Figure 6. Temperature dependence of the highest mobility 2DEG carrier.

The lowest mobility electron peak in Fig. 5 likely represents either a surface or an interface carrier in the system. The roughly temperature independent behavior of its mobility is consistent with a high-density degenerate carrier whose charge transport is dominated by impurity scattering. The small hole peaks in Fig. 5 are artifacts.

2. SdH effect measurement results

Figure 7 shows the SdH measurement result at 4.2 K. A Fourier transform analysis of these data reveals two frequencies, that yield carrier densities of $n_1=7.9 \times 10^{11} \text{ cm}^{-2}$ and $n_2=2.5 \times 10^{12} \text{ cm}^{-2}$. These two carriers agree well with the densities corresponding to the two highest mobility features in the QMSA spectra of Fig. 5. The third high mobility feature in Fig. 5 was not observed in the SdH data because of its low mobility and density (much higher field would be needed to observe the oscillation related to this carrier). The combined density of the two carriers is $3.29 \times 10^{12} \text{ cm}^{-2}$, which agrees reasonably well with the density of the broad high mobility electron peak, $3.14 \times 10^{12} \text{ cm}^{-2}$, extracted by QMSA.

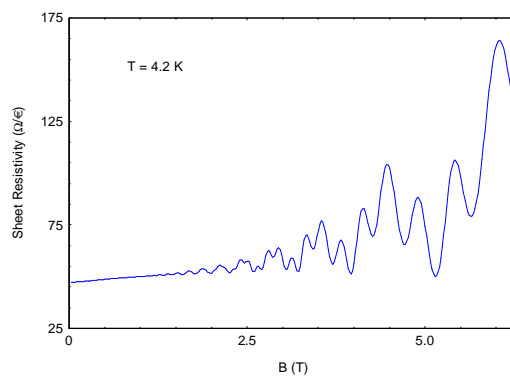


Figure 7. Multi-frequency SdH oscillation at 4.2 K.

Conclusion

We have demonstrated that variable field Hall measurements and the fully automated QMSA are capable of providing much more information than single-field data when applied to multi-carrier devices. QMSA is especially powerful in characterizing high mobility devices such as *p*HEMTs and multi quantum wells. For the present InP *p*HEMT device, QMSA easily separates the high mobility 2DEG carrier(s) from the low mobility species. The information in the separated peaks of the QMSA spectra provides an in-depth description of the transport properties of the heterostructure device. Furthermore, we have shown that QMSA is capable of probing multiple subband 2DEG carriers, which are usually investigated using quantum Hall measurements. The advantage of using variable field Hall measurements and QMSA in routine production QA/QC and device R&D for heterostructure materials, rather than conventional single-field Hall characterization methods, has been clearly demonstrated.

Acknowledgments

Work at the Naval Researcher Lab was supported in part by a Cooperative Research and Development Agreement with Lake Shore Cryotronics, Inc.

References

1. J. Antoszewski, D. J. Seymour, L. Faraone, J. R. Meyer, and C. A. Hooman, *J. Electron. Mater.* **24**, 1255 (1995).
2. J. R. Meyer, C. A. Hoffman, F. J. Bartoli, D. J. Arnold, S. Sivananthan, and J. P. Faurie, *Semicon. Sci. Technol* **8**, 805 (1993).
3. J. R. Meyer, C. A. Hoffman, J. Antoszewski, and L. Faraone, *J. Appl. Phys.* **81**, 709 (1997).
4. I. Vurgaftman, J. R. Meyer, C. A. Hoffman, D. Redfern, J. Antoszewski, L. Faraone, and J. R. Lindemuth, *J. Appl. Phys.* **84**, 4966 (1998).
5. B. J. Kelley, B. C. Dodrill, J.R. Lindemuth, G. Du, and J. R. Meyer, *Solid State Technol.* **12**, 130 (2000).
6. B. C. Dodrill, J. R. Lindemuth, B. J. Kelley, G. Du, and J. R. Meyer, *Compound Semicond.* **7**, 58 (2001).
7. W. A. Beck and J. R. Anderson, *J. Appl. Phys.* **62**, 541 (1987).
8. Z. Dziuba and M. Gorska, *J. Phys. III France* **2**, 99 (1992).
9. D. C. Look, C. E. Stutz, and C. A. Bozada, *J. Appl. Phys.* **74**, 311 (1993).
10. L. M. Roth and P. N. Argyres, *Semiconductor and Semimetals*, vol. **1**, ed. by R. K. Willardson and A. C. Beer (Academic, New York, 1966) p.159.
11. E. H. Putley, *The Hall Effect* (Butterworth, London, 1960).
12. W. A. Beck and J. R. Anderson, *J. Appl. Phys.* **62**, 541 (1987).